Title
Programmed cell death at the midline patterns ipsilateral gastrulation in the amniote

Author
Maya-Ramos, Lisandro

Publication Date
2017

Peer reviewed|Thesis/dissertation

Programmed cell death at the midline patterns ipsilateral gastrulation in the amniote

by

Lisandro Maya-Ramos

DISSERTATION

Submitted in partial satisfaction of the requirements for the degree of

DOCTOR OF PHILOSOPHY

in

Biomedical Sciences

in the

GRADUATE DIVISION

of the

UNIVERSITY OF CALIFORNIA, SAN FRANCISCO

For my parents, wife and son.

ACKNOWLEDGMENTS

It is with great joy that I write this section on behalf of my esteemed friend, Lisandro. Lisandro approached me not too long ago and kindly requested I write the acknowledgments section for his thesis dissertation. He had no special stipulations, the only request was to be candid about him and the people, who I thought, contributed to his success in seizing this degree.

The parties that should be acknowledged are the man himself, his friends and family and laboratory colleagues. Starting with Lisandro, I know him as a person of broad and diverse interests, who is seldom satisfied with the common answer. Thus, it was not surprising, to any of us who knew him, when he enrolled in a scientific path. Now at the end of the road, as the humans we are, only more is expected of him.

Lisandro's erratic behavior outside of lab could only be rectified by his lovely wife, Eva. Eva has been the linchpin in Lisandro's achievements, including the completion of this work. They have known each other for more than a decade and she has provided the serenity and stability for their lasting relationship. Now, they have a son, Vicente Bitsa, who they say is on an academic path as well. Continuing the blood line of acknowledgments: Silvia & Everardo, and Everardo & Leonardo, Lisandro's parents and siblings, respectively, are Lisandro's anchor to reality outside of academia. They are always loving and supportive. Without them, Lisandro would not be.

There are only four friends that Lisandro will probably want to acknowledge. Not because they are his only four friends, or perhaps they are, but because they are his four scientific friends. Kevin Kelly, Jeronimo Miranda, Jan Schluter and Brian Yang they

all provided him with challenging and entertaining conversations, often scientific and always exhilarating .

Lisandro's laboratory colleagues also deserve to be acknowledged, starting with Takashi Mikawa, who I hear was always supportive, always inquisitive, and always encouraging. Tom Kornberg and Shaun Coughlin, thesis committee members, were central to the achievement of this work. All Mikawa lab members, Carlos Lizama and Chris Schmith - Lisandro has mentioned that at some point in space-time they all have contributed to this work in one way or another.

I would like to conclude by sharing some thoughts that emerged in a conversation with Lisandro. We were pondering on the human capacity of learning and the ability of sharing knowledge from generation to generation. Presumably, this trait is what sets us apart from other species. Whether it is language or scientific concepts, today's discoveries will be tomorrow's basis for discovery. Yet, as astutely stated by S. Hawking: "*The greatest enemy of knowledge is not ignorance, it is the illusion of knowledge"*. Thus, rigor must be the compass in our scientific journey.

Silvio Cienfuegos

Havana, Cuba

STATEMENT REGARDING AUTHOR CONTRIBUTIONS

All experiments presented here, were designed by Takashi Mikawa and Lisandro Maya-Ramos. All experiments were performed by Lisandro Maya-Ramos.

PROGRAMMED CELL DEATH AT THE MIDLINE PATTERNS IPSILATERAL GASTRULATION IN THE AMNIOTE

Bilaterality is the predominant body plan in the animal kingdom. Cells either from the left or right side, rarely cross the body midline plane throughout life**,** as evidenced by naturally occurring bilateral gynandromorphs. However, it has been a longstanding mystery how this evolutionary conserved ipsilaterality is achieved in bilaterians, including humans. Using the chick embryo as a model, we show that extracellular matrix (ECM) and caspase-3-dependent programmed cell death (PCD) localize to the primitive streak (PS) midline, faithfully directing ipsilateral ingression through the inhibition of contralateral cellular invasion. PS midline PCD is dependent on ECM accumulation. Suppression of these components results in contralateral cellular invasion. Remarkably, induced PCD alone, without ECM, is sufficient to rescue ipsilateral gastrulation. Our findings reveal that PCD actively patterns ipsilaterality, a hitherto unknown role for this basic developmental process.

TABLE OF CONTENTS

LIST OF FIGURES

CHAPTER ONE: INTRODUCTION

Bilaterians account for 99% of all species in the animal kingdom and are characterized by a coelomic cavity, three germ layers, and an anterior-posterior, dorso-ventral and midline axes. Bilateral morphology, the property of having right and left sides, is first established during gastrulation (Martindale, Finnerty et al. 2002).

Gastrulation is the developmental process by which the germ layers, ectoderm, mesoderm and endoderm, are generated. In birds and mammals, the onset of gastrulation is defined by the appearance of the primitive streak (PS) at the posterior limit of the embryo. The PS bisects the embryonic disc in half, giving rise to morphologically distinguishable right and left sides. The process of gastrulation involves movement of dorsal epiblast cells towards the PS, where they undergo an epithelial to mesenchymal transition (EMT). Then, PS cells ingress ventrally and move away, to pattern left and right sides (Mikawa, Poh et al. 2004).

How bilaterality, or left/right patterning, is achieved is still a big unknown. However, evidence from naturally occurring “bilateral gynandromorphs” and cell-tracing experiments (Hirose and Jacobson 1979, Aw and Levin 2008) suggest that ipsilaterality, or the establishment of a boundary between right and left sides, is a key component of bilateral patterning. In bilateral gynandromorphs, one side of the animal is male and the other side is female, each side with unique phenotypic characteristics. Surprisingly, left and right sides are separated exactly by the body midline. This suggests that in development, phenotypically different left and right sides were prevented from crossing the embryonic midline. Thus, the concept of ipsilaterality denotes that the cellular

components of the right side originate from the right side with little contribution from the contralateral, or left, side and vice-versa.

In this thesis work, I address the biological principles underlying bilaterality patterning, in particular the mechanisms directing patterning of both left and right sides of the avian embryo. The motivation for this work stems from the lack of basic knowledge regarding this widespread animal trait, which is extremely familiar to us and therefore often ignored.

References

Aw, S. and M. Levin (2008). "What's left in asymmetry?" Dev Dyn **237**(12): 3453-3463.

Hirose, G. and M. Jacobson (1979). "Clonal organization of the central nervous system of the frog. I. Clones stemming from individual blastomeres of the 16-cell and earlier stages." Dev Biol **71**(2): 191-202.

Martindale, M. Q., J. R. Finnerty and J. Q. Henry (2002). "The Radiata and the evolutionary origins of the bilaterian body plan." Mol Phylogenet Evol **24**(3): 358-365.

Mikawa, T., A. M. Poh, K. A. Kelly, Y. Ishii and D. E. Reese (2004). "Induction and patterning of the primitive streak, an organizing center of gastrulation in the amniote." Dev Dyn **229**(3): 422-432.

CHAPTER TWO: PROGRAMMED CELL DEATH AT THE MIDLINE PATTERNS IPSILATERAL GASTRULATION IN THE AMNIOTE

Bilaterality is first morphologically visible at the onset of gastrulation, as the PS bisects the embryonic disc into right and left halves. Once the PS is formed, epiblast cells move to the PS and undergo ventral ingression, patterning the left and right sides (Mikawa, Poh et al. 2004). Given that bilateral, left-right, patterning starts during gastrulation, we hypothesized that ipsilaterality patterning is achieved during this process.

Discrete epiblast regions were electroporated with a DNA plasmid encoding a GFP-tagged histone, either right (Fig 1a) or left (Fig 1b) of the initial PS prior to epiblast ingression [Stage 2; Hamburger and Hamilton staging (Hamburger and Hamilton 1951)]. Embryos were then live-imaged at low magnification to capture whole-embryo cellular flow dynamics. Labeled left and right epiblast cells moved stereotypically towards the PS and underwent ingression (Fig 1c, d). The majority of cells (96% +/- SD, n=7) then moved away from the PS on the ipsilateral (same) side as the origin of transfection (Fig 1e, f). These results demonstrate that: First, ipsilateral ingression is bilateral, this is, symmetrically-present on both sides of the embryo; Second, ipsilaterality is patterned during gastrulation.

Given that PS cells undergo EMT and mesenchymal cells are known to be highly invasive (Thiery 2002), we were surprised to find that GFP labeled cells came to a halt

at the PS midline creating a sharp boundary (Fig 2a-d). The observable line of GFP cells at the PS midline suggests the presence of a midline barrier preventing cell from leaving their ipsilateral compartment. We hypothesized that PS midline cues could be involved in directing ipsilateral ingression. Therefore, we examined cellular ingression at the PS midline with increased spatiotemporal depth via biphotonic live imaging. Shortly before ingression, membrane tethered-GFP labeled cells directed an increased number of projections towards the PS midline, (Fig 2e, f) implicating the PS midline as a potential regulator in preventing contralateral invasion.

To rule out the possibility that ipsilateral ingression is due to information inherent to epiblast cells, we performed classical chimeric experiments (Fig 3a, b). Isochronic epiblast grafts from transgenic GFP chick embryos were placed on the contralateral side of GFP negative embryos and live imaged (Fig 3c, d). If ipsilateral ingression is determined by inherent information in the epiblast, we would expect cells to ingress to the contralateral side, representing their original starting position. However, grafted cells (93% +/-) displayed ipsilateral ingression, following the same trajectory as the native neighboring cells, similar to control experimental grafts (Fig 3e, f). These data suggest that ipsilateral ingression is not epiblast dependent, thus we centered our attention on the PS midline.

The PS midline has been previously defined by a combination of cellular and molecular characteristics, including those known to regulate cell migration, proliferation and survival (Kelly, Wei et al. 2002, Yang, Dormann et al. 2002, Wolf, Te Lindert et al. 2013). Therefore we took a candidate approach in looking for potential molecules involved in ipsilateral ingression. Specifically, we surveyed PS midline expression of axonal

guidance cues, extracellular matrix (ECM) constituents, growth factors and programmed cell death (PCD) (Fig 4).

From the candidate list, we focused our attention on PCD. To our knowledge, in embryonic development, PCD is followed by cellular corpse clearance (Lauber, Blumenthal et al. 2004). However, we found an unusual enrichment of PCD present at the PS midline, using three different methods; propidium iodide staining (Fig 4f), cleaved caspase-3 immuno-fluorescence (IF) staining (Fig 5b-e), and scanning electron microscopy (S.E.M) (Fig 5a). This enrichment could be due to the lack of specialized scavenging cells and/or it could be related to a novel biological function of PCD. To explore this, we experimentally tested the latter possibility, as macrophages are not yet formed during gastrulation. To inhibit PCD, the pan-caspase inhibitor, P35 protein from baculovirus, was used (Sugimoto, Friesen et al. 1994). To trace cells expressing the P35 inhibitor, a DNA construct was created where P35 was linked via the viral cleaving peptide 2A to GFP labeled histone: P35-2A-H2B:GFP, from hereafter P35. P35 PS midline expression resulted in loss of P.I. staining, suggesting that over expression was functionally eliminating cell death (Fig 5g). We then RFP labeled wild type (WT) epiblast cells lateral to the PS while over-express ing P35 at the PS midline, in the same embryo (Fig 5f). 35% of the WT-RFP labeled cells invaded the contralateral side in comparison to 4% in control embryos (Fig 5h, i). These results suggest that PCD is necessary to prevent cellular contralateral invasion.

On the basis of this data, we searched for potential PCD regulators involved in ipsilateral ingression. We started by probing FGF8 from our candidate list (Fig 4e), since it is a potent mitogenic, is expressed at the PS midline and is a presumed repulsive

signal (Yang, Dormann et al. 2002). Overexpression of an FGFR1 dominant negative receptor (Fig 6a), FGFR1-2A-H2B:GFP, from hereafter DN-FGFR1, diminished T gene expression (Fig 6b) as previously reported (Stuhlmiller and Garcia-Castro 2012), confirming that the construct, was biologically active as a dominant negative effector of the signaling cascade. However, DN-FGFR1 expressing cells underwent ipsilateral ingression similar to wild type (WT) embryos (Fig 6c, d, 1e, f). These results indicate that FGF8 signaling is not required for ipsilateral ingression.

Guided by two lines of evidence, we then turned to test the role of ECM in PCD regulation and ipsilateral ingression. First, high ECM density alone can block cellular migration (Wolf, Te Lindert et al. 2013) and loss of or inappropriate cell-to-ECM contact can result in PCD (Taddei, Giannoni et al. 2012). ECM-basement membrane (BM) constituents, laminin, fibronectin and collagen type IV, were present as a continuous line of signal just basal to the epiblast, then fenestrated at the lateral PS site of cellular ingression, and highly enriched at the PS midline (Fig 7a-c). This expression pattern suggests that ECM-BM is regulated by factors, that may prevent PS midline ECM fenestration, as in lateral PS. We found expression of the membrane-bound matrix metalloproteinase-15 (MMP-15) in lateral PS, and tissue inhibitor of metalloproteinase-3 (TIMP-3) in PS midline (Fig 5d-f). These results suggest a spatially restricted ECM regulation, whereby MMP-15 activity is confined to lateral PS areas, to allow for cellular ingression, and inhibited by TIMP-3 at the PS midline, resulting in PS midline ECM enrichment.

We next probed the necessity of PS midline ECM in ipsilateral ingression. Based on our observation that MMP-15 expression is reduced at the PS midline, we ectopically

expressed human MMP-15-2A-mCherry, from hereafter hMMP-15, at this site. Ectopic expression of hMMP-15 at the PS midline successfully decreased PS midline ECM protein enrichment (Fig 7h). Ectopic expression of hMMP-15 at the PS midline in embryos with GFP labeled WT epiblast cells (Fig 7g), resulted in 40% of GFP-WT cells invading the contralateral side as compared to 4% in control embryos (Fig 7i, j, 1e, f). To exclude the possibility that contralateral ingression was due to off-target effects of hMMP-15, we confirmed these results, by specifically targeting the laminin alpha-1 (LAMA1) gene via morpholino. LAMA1 morpholino, knocked down laminin expression in contrast to the scramble morpholino control (Fig 8a-d). PS LAMA1 morpholino introduction resulted in 20% cells crossing the midline (Fig 8e, f). Although LAMA1 morpholino expression led to a smaller percentage of cells crossing the midline, this result was expected, as MMP-15 is an ECM protease, whereas LAMA1 morpholino only targeted the laminin protein. Thus, this results substantiates the concept that ECM is necessary for preserving ipsilateral ingression.

In light of both PCD and ECM preventing contralateral invasion, we interrogated the relationship between these two components. Detailed I.F. staining analysis revealed that cleaved caspase-3 and ECM laminin are found to be adjacent to each other (Fig 9a-c). This suggests that there could be a regulatory interaction between the two, thus we assessed ECM levels under PCD inhibition and vice-versa. PS midline PCD inhibition by P35 did not alter the ECM pattern of laminin (Fig 9d-f). Given that this challenge leads to contralateral ingression, these results suggest that ECM alone is not sufficient to dictate ipsilateral ingression. At variance with this finding, morpholino mediated PS midline laminin knock down diminished the overall level of cleaved caspase-3 signal at

the PS, when compared to morpholino control and WT embryos (Fig 9g), suggesting a link between ECM and PCD. These data, however, do not distinguish whether ECM or PCD is sufficient to prevent contralateral cellular invasion.

To unambiguously test PCD sufficiency in ipsilateral ingression, we traced cellular ingression in embryos with knock-down PS midline laminin while ectopically inducing PCD. If PCD is sufficient to induce ipsilateral ingression, then in embryos without PS midline laminin, which leads to contralateral invasion, ectopic PCD should rescue ipsilateral ingression. Thus we tested this by using the kinase inhibitor, staurosporine, known to cause cellular apoptosis (Fig 9h) (Belmokhtar, Hillion et al. 2001). Remarkably, staurosporine-induced PCD was sufficient to rescue ipsilateral ingression (Fig 9i) in an ECM diminished background (Fig 9k). Even more compelling, ipsilateral ingression was localized only to the site of induced PCD, whereas contralateral ingression occurred at PS regions without PCD (Fig 9l). Altogether, these results demonstrate that ECM and PCD are required to precisely pattern bilateral ipsilateral ingression, yet, sufficiency is only achieved by PCD.

References

Belmokhtar, C. A., J. Hillion and E. Segal-Bendirdjian (2001). "Staurosporine induces apoptosis through both caspase-dependent and caspase-independent mechanisms." Oncogene **20**(26): 3354-3362.

Hamburger, V. and H. L. Hamilton (1951). "A series of normal stages in the development of the chick embryo." J Morphol **88**(1): 49-92.

Kelly, K. A., Y. Wei and T. Mikawa (2002). "Cell death along the embryo midline regulates left-right sidedness." Dev Dyn **224**(2): 238-244.

Lauber, K., S. G. Blumenthal, M. Waibel and S. Wesselborg (2004). "Clearance of apoptotic cells: getting rid of the corpses." Mol Cell **14**(3): 277-287.

Mikawa, T., A. M. Poh, K. A. Kelly, Y. Ishii and D. E. Reese (2004). "Induction and patterning of the primitive streak, an organizing center of gastrulation in the amniote." Dev Dyn **229**(3): 422-432.

Stuhlmiller, T. J. and M. I. Garcia-Castro (2012). "FGF/MAPK signaling is required in the gastrula epiblast for avian neural crest induction." Development **139**(2): 289-300.

Sugimoto, A., P. D. Friesen and J. H. Rothman (1994). "Baculovirus p35 prevents developmentally programmed cell death and rescues a ced-9 mutant in the nematode Caenorhabditis elegans." EMBO J **13**(9): 2023-2028.

Taddei, M. L., E. Giannoni, T. Fiaschi and P. Chiarugi (2012). "Anoikis: an emerging hallmark in health and diseases." J Pathol **226**(2): 380-393.

Thiery, J. P. (2002). "Epithelial-mesenchymal transitions in tumour progression." Nat Rev Cancer **2**(6): 442-454.

Wolf, K., M. Te Lindert, M. Krause, S. Alexander, J. Te Riet, A. L. Willis, R. M. Hoffman, C. G. Figdor, S. J. Weiss and P. Friedl (2013). "Physical limits of cell migration: control by ECM space and nuclear deformation and tuning by proteolysis and traction force." J Cell Biol **201**(7): 1069-1084.

Yang, X., D. Dormann, A. E. Munsterberg and C. J. Weijer (2002). "Cell movement patterns during gastrulation in the chick are controlled by positive and negative chemotaxis mediated by FGF4 and FGF8." Dev Cell **3**(3): 425-437.

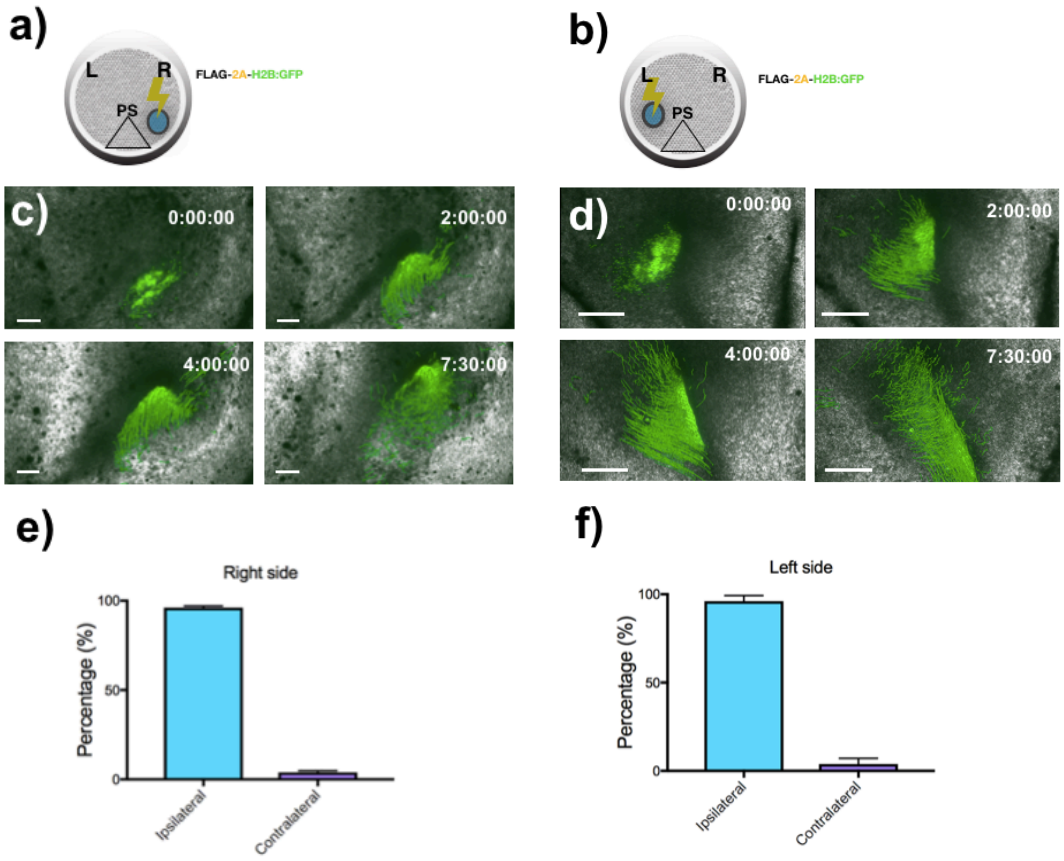

Figure 1. Ipsilateral ingression is bilateral and patterned in gastrulation: a) Scheme of right side epiblast H2B-GFP electroporation at stage HH2. b) Scheme of left side epiblast H2B-GFP electroporation at stage HH2. c) Representative time-lapse still images of right side epiblast electroporation during gastrulation, scale bar 500µm. d) Representative time-lapse still images of left side epiblast electroporation during gastrulation. e) Right side quantification of H2B-GFP labeled cells that underwent ingression, 96.14% ipsilateral versus 3.857% (SEM ± 0.338, n=7) contralateral ingression. f) Left side quantification of H2B-GFP labeled cells that underwent ingression, 96.09 % ipsilateral and 3.914% (SEM ± 1.218 n=7) contralateral ingression.

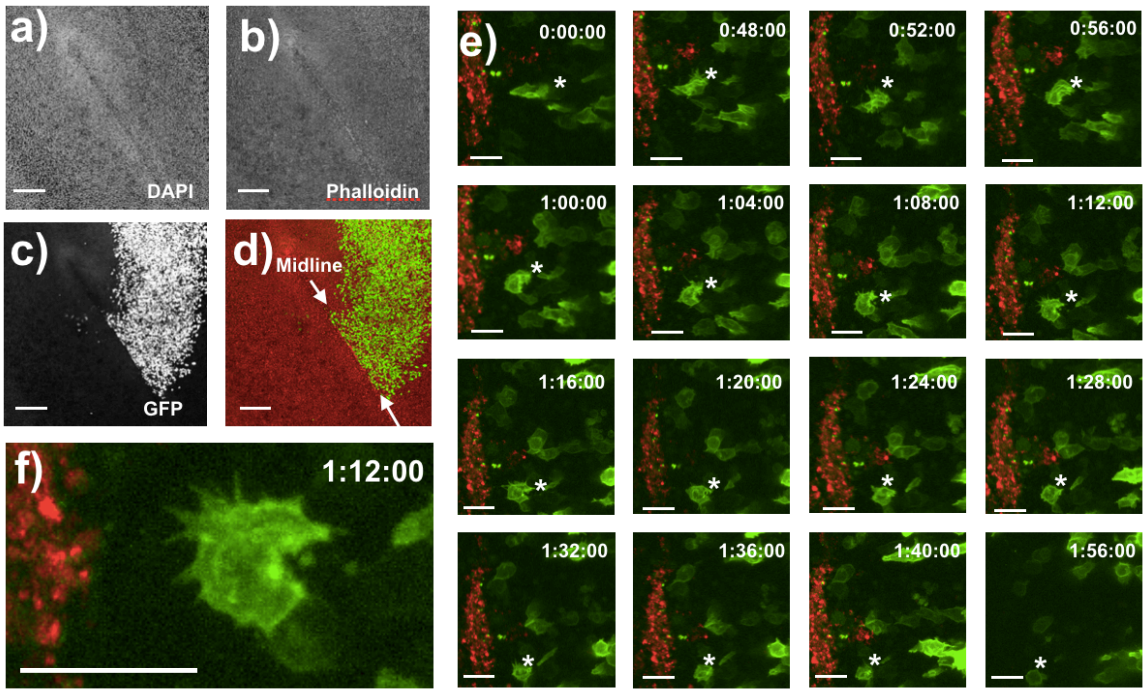

Figure 2. PS midline association with cellular projections from ingressing cells: a, b, c, d) Superior view of GFP electroporated embryo, scale bar 200μm. a) DAPI staining. b) Phalloidin staining. c) GFP electroporated cells. c) Merged phalloidin and GFP images, note sharp line of GFP labeled cells at PS midline (white arrows). e) Biphotonic time-lapse still images of membrane-tethered GFP electroporated cells. Asterisks indicates cell approaching PS midline (stained with red propidium iodide). Notice that at time 0:00:00 hours, there are no visible cellular projections, however at time 0:52:00 hours cellular projections are oriented towards PS midline, scale bar 20μm. f) Time-lapse 1:12:00 still image of cells with multiple projections oriented towards PS midline, scale bar 20μm.

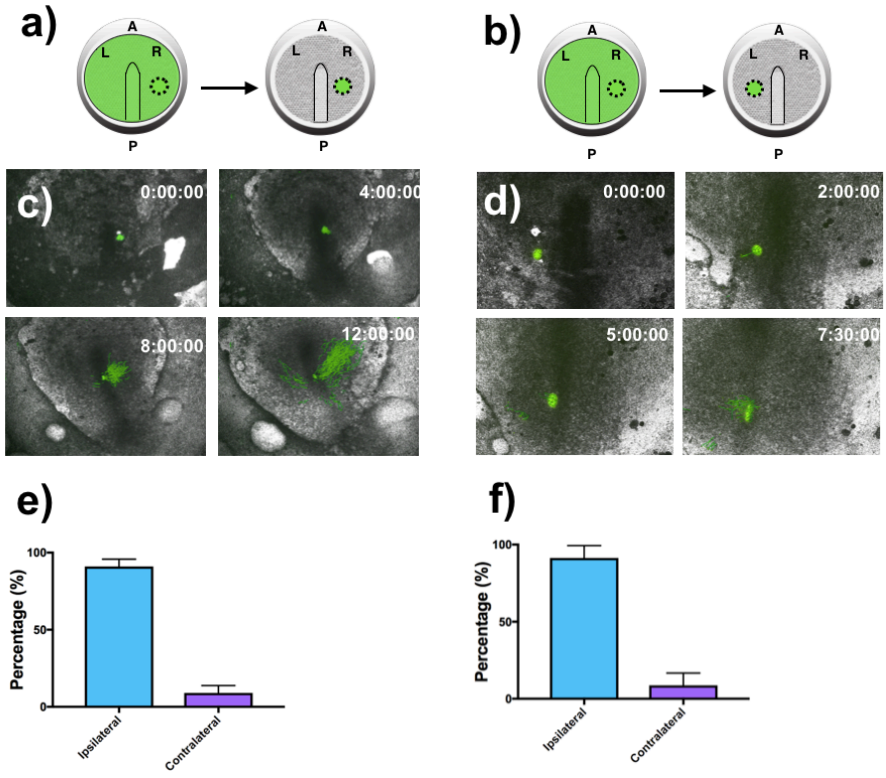

Figure 3. Heterotopic isochronic graft undergo ipsilateral ingression: a) Scheme depicting a homotopic and isochronic graft. b) Scheme depicting a heterotopic and isochronic graft. c) Representative time-lapse still images of homotopic graft during gastrulation. d) Representative time-lapse still images of heterotopic graft during gastrulation. e) Homotopic graft ingression quantification 91% ipsilateral versus 9% (SEM ± 2.414, n=4) contralateral ingression. F) Heterotopic graft ingression quantification 91.33 % ipsilateral and 8.667% (SEM ± 4.667 n=3) contralateral ingression .

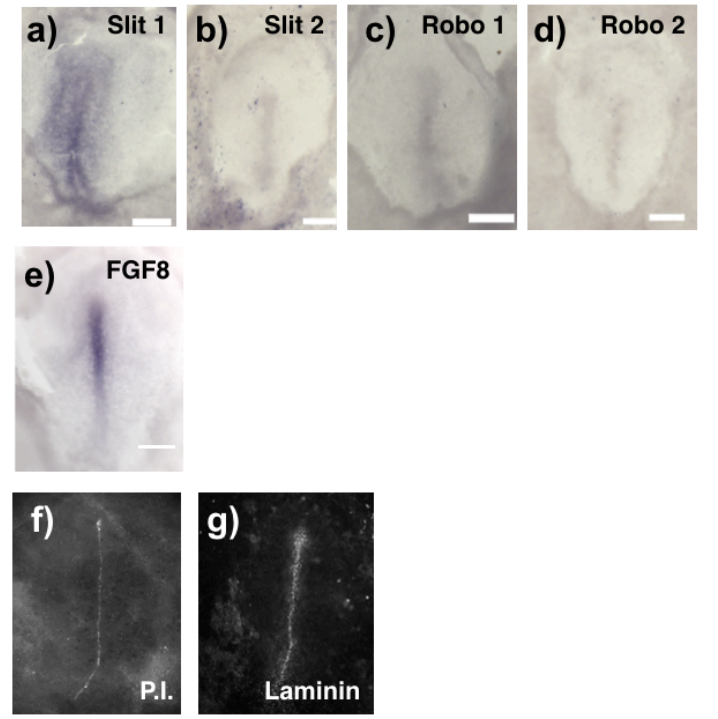

Figure 4. FGF8, propidium iodide and laminin are expressed at the PS midline: a) In situ hybridization (ISH) of Slit 1, with PS expression, scale bar 400μm. b) Slit 2 ISH, scale bar 400μm. c) Robo 1 ISH, scale bar 400μm. d) Robo 2 ISH, scale bar 400μm. e) FGF8 ISH, scale bar 400μm. f) Propidium iodide staining of PS midline. g) Laminin IF. staining, showing enrichment at the PS midline.

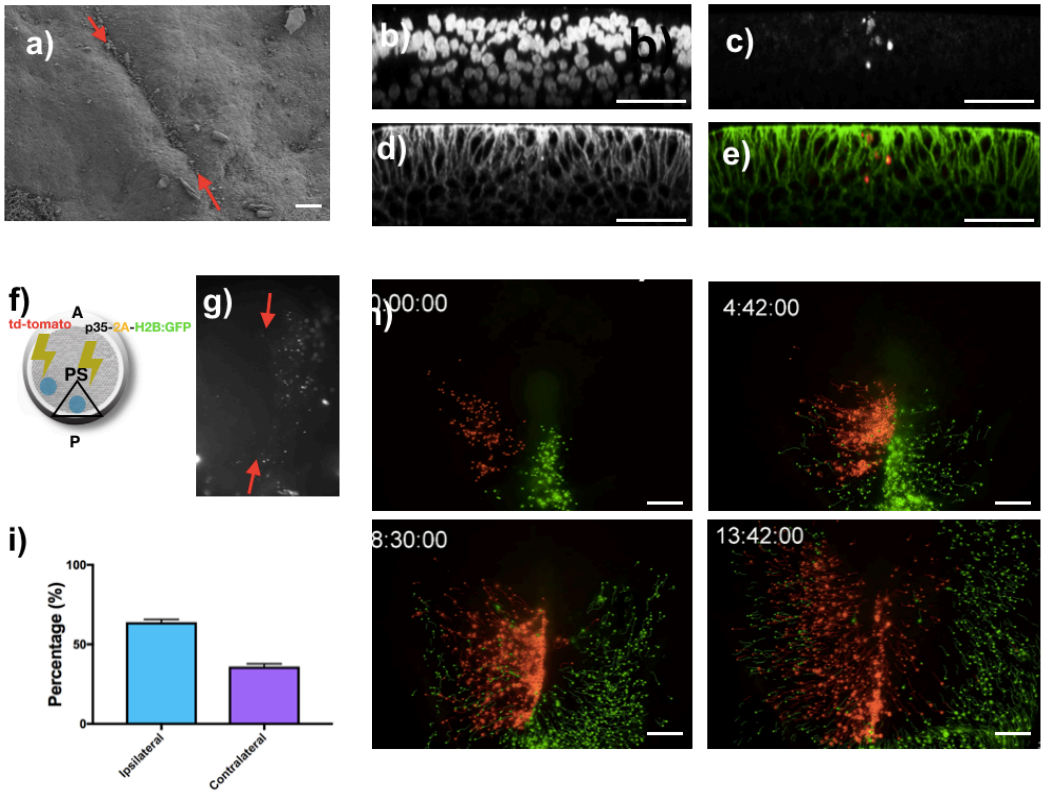

Figure 5. PS midline programmed cell death loss results in cellular contralateral invasion: a) Scanning electron image of stage HH 3 embryo, showing cellular-like debris at the PS midline (red arrows), scale bar 40µm. b, c, d, e) Cross section of stage HH 3 embryo, scale bar 50µm. b) DAPI staining. c) Cleaved caspase-3 IF staining. d) Phalloidin staining. e) Merged phalloidin (green) and cleaved caspase-3 (red) images. f) Scheme of stage HH 2 embryo double-electroporated with td-Tomato on lateral left epiblast and the pan-caspase P35 inhibitor linked to viral 2A peptide and H2B:GFP at the PS midline. g) Propidium iodide staining of p35 PS midline electroporated embryo. Notice absence of signal between red arrows. h) Representative time lapse still images of td-tomato electroporated left epiblast and P35-2A-H2B:GFP PS midline, scale bar 300µm. i) Ingression quantification of td-tomato that underwent ingression in P35 electroporated embryos, 63.96 % ipsilateral and 36.04% (SEM ± 1.012 n=3) contralateral ingression.

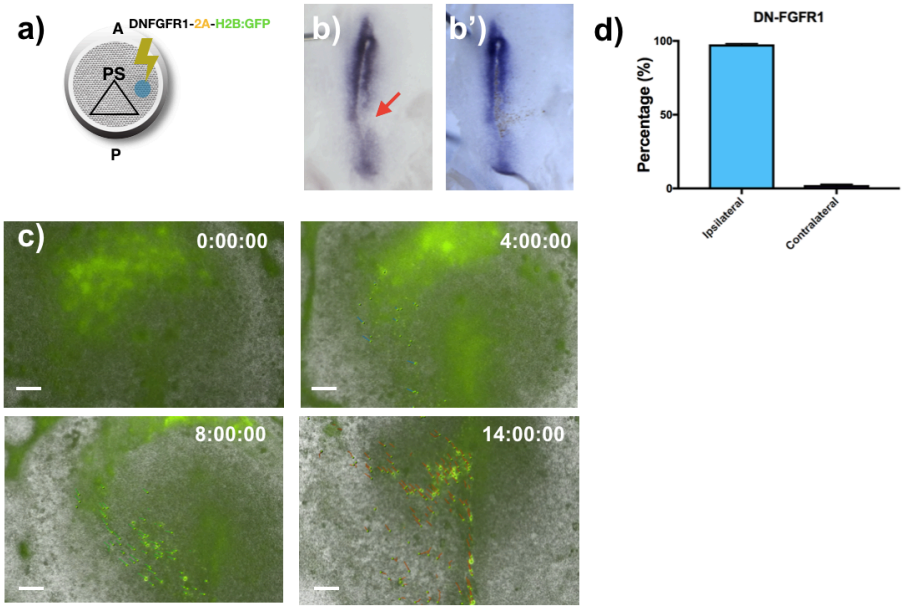

Figure 6. DN-FGFR1 expressing cells undergo ipsilateral ingression: a) Scheme of stage HH 2 embryo electroporated with an FGFR1 dominant negative linked to viral 2A peptide and H2B:GFP on lateral epiblast. b) Brachyury ISH of DN-FGFR-2A-H2B:GFP electroporated embryo, note lack of brachyury signal on electroporated side (red arrow). b') Horse radish peroxidase (brown signal) showing DN-FGFR1-2A-H2B:GFP electroporated cells. c) Representative time lapse still images of DN-FGFR1 electroporated right epiblast, note that after 14:00:00 hours, most cells underwent ipsilateral ingression, scale bar 300µm. d) Ingression quantification of DNFGFR1-2A-H2B:GFP electroporated embryos, 97.67 % ipsilateral and 2.333% (SEM ± 0.3333 n=3) contralateral ingression .

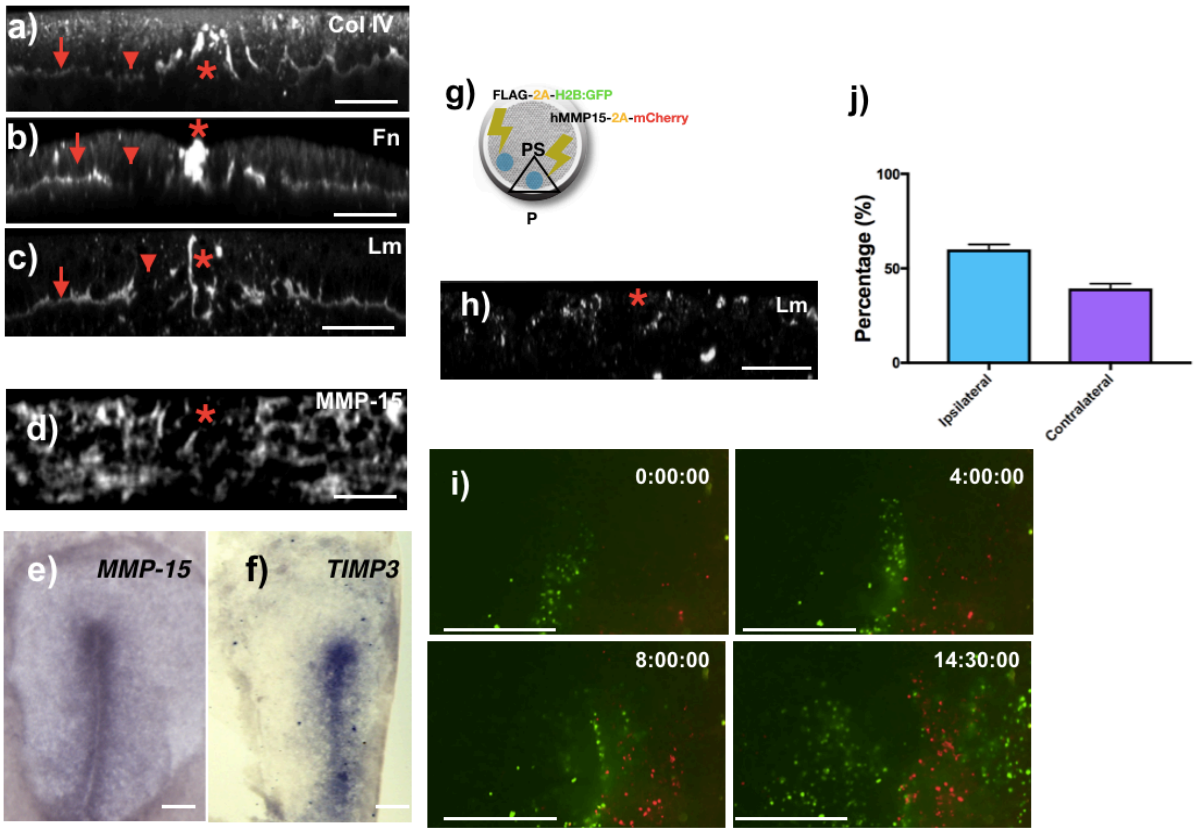

Figure 7. PS midline extracellular matrix loss results in cellular contralateral invasion: a) Cross section of collagen type IV I.F. stained embryo, scale bar 50um. b) Cross section of fibronectin I.F. stained embryo, scale bar 50um. c) Cross section of laminin I.F. stained embryo, scale bar 50um. a, b, c) Arrow points to continuous line of signal ECM-BM, arrowhead shows fenestrated ECM-BM and asterisks denotes enrichment of ECM-BM at PS midline. d) Cross section of membrane bound MMP-15 I.F. stained embryo, asterisks denotes decreased PS midline signal, scale bar 50um. e) MMP-15 ISH, scale bar 300um. f) TIMP3 ISH, scale bar 300um. g) Scheme of stage HH 2 embryo double-electroporated with Flag-2A-H2B:GFP on lateral left epiblast and human MMP-15 linked to viral 2A peptide and H2B:GFP at the PS midline. h) Cross section of laminin I.F staining in PS midline MMP-15 electroporated embryo, asterisks denotes decreased PS midline signal, scale bar 50um. i) Representative time lapse still images of FLAG-2A-H2B:GFP electroporated left epiblast and hMMP15-2A-H2B:GFP PS midline, scale bar 500µm. j) Ingression quantification of FLAG-2A-H2B:GFP that underwent ingression in hMMP15 electroporated embryos, 60 % ipsilateral and 40% (SEM ± 1.528 n=3) contralateral ingression.

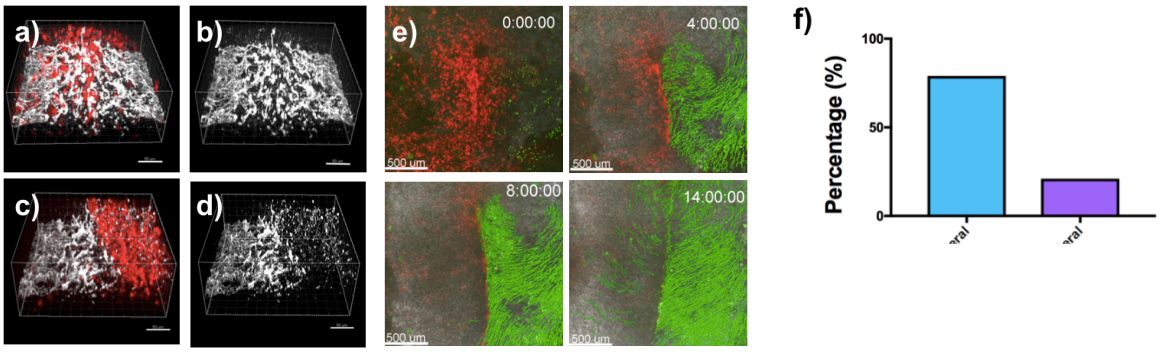

Figure 8. PS midline laminin loss results in contralateral cellular ingression: a, b) LAMA1 translation blocking control morpholino linked to lissamine and laminin I.F. stained embryo. a) Merged LAMA1-control-lissamine morpholino and laminin, scale bar 50um. b) Laminin I.F. staining, scale bar 50um. c, d) LAMA1 translation blocking morpholino linked to lissamine and laminin I.F. stained embryo. c) Merged LAMA1-lissamine morpholino and laminin, scale bar 50um. d) Laminin I.F. staining, scale bar 50um. e) Representative time lapse still images of FLAG-2A-H2B:GFP electroporated left epiblast and LAMA1-lissamine morpholino PS midline, scale bar 500µm. j) Ingression quantification of FLAG-2A-H2B:GFP that underwent ingression in LAMA1-lissamine morpholino electroporated embryos, 80 % ipsilateral and 20% contralateral ingression.

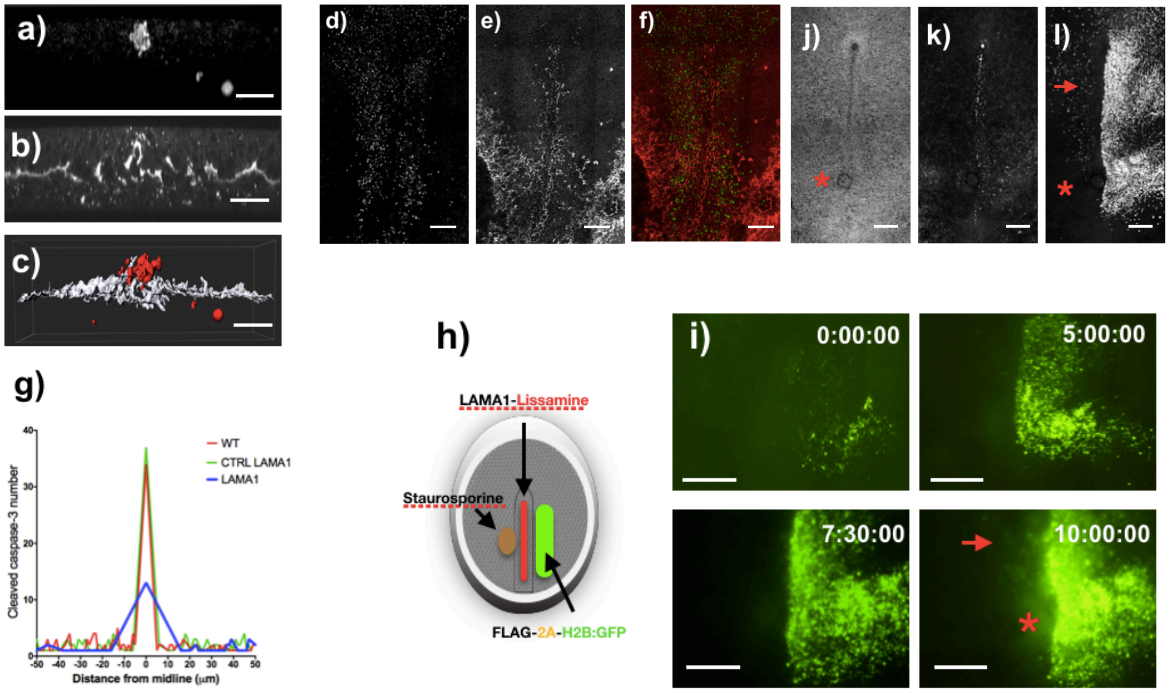

Figure 9. Ectopic induced programmed cell death rescues ipsilateral ingression: a) Cross section of cleaved caspase-3 I.F. staining, scale bar 50um. b) Cross section of laminin I.F. staining, scale bar 50um. c) Merged 3D reconstruction of a and b. Laminin shown in white and cleaved caspase-3 in red, scale bar 50um. d) PS P35-2A-H2B:GFP electroporated embryo, scale bar 300 um. e) Laminin I.F. staining in P35-2A-H2B:GFP electroporated embryo, scale bar 300 um. f) Merged d and e, laminin (red) and P35-2A-H2B:GFP (green), scale bar 300 um. g) Cleaved caspase-3 cluster number (I.F. staining) in wild-type, control LAMA1 morpholino and LAMA1 morpholino. In X axis, 0 represents midline. h) Scheme of stage HH 3 showing rescue experiment, with PS midline LAMA1-lissamine expression and lateral FLAG-2A-H2B:GFP in right lateral epiblast, with left epiblast staurosporine microinjection. i) Representative time lapse still images of FLAG-2A-H2B:GFP electroporated right epiblast in LAMA1-lissamine PS midline, arrow points to contralateral ingression while asterisk denotes site of staurosporine injection (0.3mM) with no visible contralateral ingression, scale bar 500μm. j) DAPI stained embryo, from panel i, asterisk shows site of staurosporine microinjection, scale bar 300 um. k) Laminin I.F. stained embryo, from panel i, PS midline laminin enrichment is decreased, scale bar 300 um. l) GFP stained embryo, from panel i, arrow points to cells found on the contralateral side of original electroporation, asterisk shows site of staurosporine microinjection, scale bar 300 um.

CHAPTER THREE: CONCLUSIONS

I have presented here evidence for the existence of an early developmental mechanism ensuring ipsilateral ingression patterning, dependent primarily on PCD. To our knowledge these data advance the concept that ipsilaterality is a fundamental developmental component of amniotes and quite possibly of all bilaterians. This suggests that left and right sides are patterned as two separate compartments, with minimal mixing between them. Interestingly, in humans, ipsilaterality is most exaggerated during pathological processes, such as in the case of congenital hemiplegia, where one half of the body is paralyzed and the body midline is the boundary of healthy and affected sides (Aw and Levin 2008).

From a cell biological point of view, the data presented here suggest that PCD is sufficient to change the direction of migrating cells. This is a novel function for a very well established developmental process such as PCD. In ipsilaterality patterning, PCD acts as a barrier to prevent cellular invasion to the contralateral side. More work is needed, however, to elucidate whether chemical or physical PCD elements are directly involved in altering cell migration during gastrulation.

In conclusion, we have discovered that ipsilaterality is a fundamental process of bilateral gastrulation. ECM and PCD provide a framework of ipsilaterality patterning, where first ECM is spatially regulated by MMP-15 and TIMP-3, resulting in an enrichment of ECM at the PS midline. ECM then leads to PS midline PCD accumulation, which ultimately prevents cells from invading the contralateral side.

References

Aw, S. and M. Levin (2008). "What's left in asymmetry?" Dev Dyn **237**(12): 3453-3463.

CHAPTER FOUR: PROTOCOLS

Protocol 1: Embryo handling and live imaging

Fertilized chicken (Gallus gallus domesticus) eggs were obtained from a local breeder (Petaluma Farms, CA) and incubated in a humid incubator at 37°C until Hamburger Hamilton stage (HH) 2. For ex-vivo manipulations, embryos were isolated in Pannett-Comptons solution [40mL of solution A, 60 mL of solution B in 1L of H2O final volume. Solution A: 121 g NaCl, 15.5 g KCl, 10.42 g CaCl 2–2H 2O, and 12.7 g MgCl 2–6H 2O in 1L of H2O final volume. Solution B: 1.88 g Na 2HPO 4, and 0.188 g NaH 2PO 4–2H 2O in 1L of H2O final volume.] under a Seizz Stemi 2000C stero microscope and cultured according to the New Culture method (New, 1955) . Embryos in New Culture were time-lapse imaged with either: Nikon Eclipse TE2000-E supported by Hamamatsu ORCA-Flash 2.8 camera or Nikon Eclipse Ti supported by ANDOR iXon camera, with a 4X objective using Nikon Elements Advance Research software V4.00.07. For bi-photonic imaging, embryos were culture with a modified version of New Culture technique, 100 µL of substrate mix of albumin and 2% agar, was added to a glass-bottom 35mm culture plate. Time-lapse images were acquired every 3-4 minutes with a Zeiss LSM 7 MP, W Plan-APOCHROMAT 2-photon microscope (using 20x/1.0 objective), equipped with a Non-descanned detector PMT, and ZEN 2012 SP2 (black) software.

Protocol 2: Electroporation, DNA constructs and morpholinos

HH2 embryos were isolated in Pannett Compton Solution and placed dorsal side up on an electroporating chamber containing Tyrodes solution [137mM NaCl, 2.7 mM KCL, 1mM MgCl2, 1.8mM CaCl2, 0.2 mM Ha2HPO4, 5.5mM D-glucose, 15mM Hepes, pH 7.4]. DNA mix (DNA 3µL, H2O 1.5µL, FastGreen 0.5µL and 60% sucrose 0.5µL) was added to dorsal epiblast, and embryos were electroporated at 3.5 volts, 50 milliseconds pulse, 500 milliseconds intervals, and 3 times using the NEPA 21 Super Electroporator Type II. Embryos were then cultured for subsequent experimentation.

The CAG plasmid, gift from Dr. Connie Cepko (Addgene plasmid # 11150) was used as a backbone for Gibson Assembly (New England Biolabs, Ipswich, Massachusetts) cloning of: FLAG-2A-H2B:GFP; P35, a gift from Dr. Patrick Mehlen; MMP15 (NM_002428.2) , MMP15-2A-mCherry and MMP15-2A-H2B:GFP, (Vector Builder, Santa Clara, California). pCCALL2 DN-FGFR1-IRES-EGFP, a gift from Dr. Gerard Blobbe. Membrane GFP, pCAGS-GAP43-GFP, a gift from Dr. Orion Weiner. Translation blocking 3' Lissamine LAMA1 (NM_001199806.1) morpholino (5'-CCCATCACCATCGCCGCCAC-3') (Gene Tools, Philomath, Oregon, USA) and five-mispair sequence control (5'-CCGATCACGATCCCCCCGAC-3') were electroporated as previously indicated.

Protocol 3: Immunofluorescence staining and scoring

Embryos were harvested from egg yolk and placed on 1X PBS, then fixed in 4% paraformaldehyde in PBS for 0.5 hours at room temperature, followed by 0.5 hours of PBS washing. Blocking media, (1% BSA, 0.1% triton in PBS) was added for 1 hour at room temperature, followed by primary antibody staining. Primary antibodies were added in blocking solution overnight at room-temperature, followed by 2 hours of PBS washing. Secondary antibodies were added in blocking solution for 2 hours followed by 2 hours of PBS washing with DAPI (1:1000). Embryos were mounted dorsal side up in mounting media. Antibodies used: laminin (1:400) 3H11-S anti-mouse and fibronectin (1:400) anti-rabbit B3/D6-C (Developmental Studies Hybridoma Bank, Iowa City, Iowa), MMP-15 (1:150) anti-rabbit ab15475 and Collagen IV (1:200) anti-rabbit ab6586 (Abcam, Cambridge, United Kingdom), Cleaved caspase-3 (1:150) anti-rabbit 9661S (Cell Signaling Technologies, Danvers, Massachusetts). GFP anti-rabbit (1:400) A11122, Alexa Fluor 488 (1:500) anti-rabbit A11008, Alexa Fluor 488 (1:500) anti-mouse A11001, Alexa Fluor 594 (1:500) anti-mouse A21203, Alexa Fluor 594 (1:500) anti-rabbit A11037, Alexa Fluor 647 (1:500) anti-mouse A31571 (Thermo Fisher, Waltham, Massachusetts).

Scoring of cellular ingression was done in H2B-GFP and laminin double stained embryos. In the Imaris X64 9.0.2 version**,** first a surface mask was created using laminin as a basement membrane marker, to exclude epiblast and only analyze the cells that underwent ingression. Then, the spot function was employed to count all H2B-GFP positive cells on each side of the primitive streak. Total percentage included cells from both right and left ventral sides. Left and right percentage were calculated by dividing the number of cells from that side over the sum of both sides.

Protocol 4: In situ hybridization and HRP staining

Embryos were fixed overnight at 4 degrees celsius in 4% paraformaldehyde, then washed in PBT for 30 minutes, followed by proteinase K (1:2000) in PBT treatment for 1 minute at room-temperature. Then, embryos were treated with glycine (2mg/mL) in PBT for 20 minutes and then washed with PBT for 10 minutes. Embryos were incubated at 70 degrees celsius for 2 hours in pre-hybridization buffer (10mL solution 1 (1% SDS, 5X SSC, 50% formamide), 10µL of heparin (50µg/mL), 50µL yeast RNA (50µg/mL)) followed by overnight probe incubation at 70 degrees celsius. Next, the probe was replaced by solution 1 and washed twice 30 minutes each. Then, washed twice with solution 3 (50% formamide and 2X SCC pH 4.5) 30 minutes each. Followed by 15 minutes of TBST washing at room temperature and blocking with 10% sheep serum in TBST for 1.5 hours at room temperature. Lastly, embryos were incubated overnight at 4 degrees celsius with DIG-Fab antibody (1:2000) in blocking solution. Next, embryos were washed for 30 minutes four times with TBST at room-temperature, followed by a 10 minute wash with NTMT (2.5mL NaCl, 1mL Tris-HCl, 1ml MgCl2, 100µL Tween and 6.4mL H2O). Development of signal was done with 4.5µL NBT and 3.5µL BCIP in 1mL of NTMT. Once signal was visible, embryos were washed in PBT and stored in 4% paraformaldehyde. GFP-HRP antibody was used for GFP detection in in-situ hybridization processed embryos. Embryos were washed in PBT, then fixed in 4:1 methanol/DMSO overnight at 4 degrees celsius, then incubated for 2 hours at room-temperature with 4:1:1 methanol/DMSO/30% H2O2 followed by 1 hour blocking at room-temperature with 1% sheep serum in TBST. The anti-GFP(HRP) antibody was added overnight in blocking media. Next, embryos were washed five times, 1 hour each,

with TBST at 4 degrees celsius, then washed 10 minutes with 0.05M Tris-HCl pH 7.6 followed by a 30 minute incubation in the dark with DAB in Tris-HCl pH 7.6. Signal was developed with DAB in Tris-HCl with 0.0003% H2O2. Images were acquired on a Leica MZ16F microscope equipped with Leica DFC300 Fx camera and Leica FireCam V.3.4.1 software. Probes used were T, FGF8, FGFR1, TIMP3, MMP-15, SLIT, ROBO.

Protocol 5: Propidium iodide staining and staurosporine micro-injections

For in-ovo propidium iodide #P3566 (Life technologies, Carlsbad, California) staining, propidium iodide (1mg/mL) was back loaded into a pulled glass micro-pipette and then micro-injected with an Ependorf Femtojet injection system in the space between the vitelline membrane and the area pellucida. Embryos were incubated for 3-5 minutes at room temperature then imaged. For staurosporine S4400 (Sigma Aldrich, St. Louis, Missouri) injection treatment, pulled glass micro pipette were back loaded with 0.9 µL of 0.3mM staurosporine, 0.5 µL fast green and 1.6 µL PBS, and embryos in New Culture were ventrally injected. All injections were recorded using a Lecia MZ16 Fluorescent stereo microscope on a Jenoptik ProgMF cool digital camera.

References

New, D.A.T. (1955) A new technique for the cultivation of the chick embryo in vitro. J. Embryol. exp. Morph. 3, 326-331.

Publishing Agreement

It is the policy of the University to encourage the distribution of all theses, dissertations, and manuscripts. Copies of all UCSF theses, dissertations, and manuscripts will be routed to the library via the Graduate Division. The library will make all theses, dissertations, and manuscripts accessible to the public and will preserve these to the best of their abilities, in perpetuity.

Please sign the following statement:

I hereby grant permission to the Graduate Division of the University of California, San Francisco to release copies of my thesis, dissertation, or manuscript to the Campus Library to provide access and preservation, in whole or in part, in perpetuity.

Author Signature

12-12-17

Date